British Journal of Pharmacology

British Journal of Pharmacology (2018) **175** 3832–3843 3832

RESEARCH PAPER

Fingerprints of CNS drug effects: a plasma neuroendocrine reflection of D_2 receptor activation using multi-biomarker pharmacokinetic/pharmacodynamic modelling

Correspondence Elizabeth CM de Lange, Division of Systems Biomedicine and Pharmacology, Leiden Academic Center for Drug Research, Leiden University, Leiden, The Netherlands. E-mail: ecmdelange@lacdr.leidenuniv.nl

Received 2 January 2018; **Revised** 6 July 2018; **Accepted** 11 July 2018

Willem J van den Brink[1], Dirk-Jan van den Berg[1], Floor E M Bonsel[1], Robin Hartman[1], Yin-Cheong Wong[1], Piet H van der Graaf[1,2] and Elizabeth C M de Lange[1]

[1]*Division of Systems Biomedicine and Pharmacology, Leiden Academic Center for Drug Research, Leiden University, Leiden, The Netherlands, and* [2]*Certara QSP, Canterbury Innovation House, Canterbury, UK*

BACKGROUND AND PURPOSE

Because biological systems behave as networks, multi-biomarker approaches increasingly replace single biomarker approaches in drug development. To improve the mechanistic insights into CNS drug effects, a plasma neuroendocrine fingerprint was identified using multi-biomarker pharmacokinetic/pharmacodynamic (PK/PD) modelling. Short- and long-term D_2 receptor activation was evaluated using quinpirole as a paradigm compound.

EXPERIMENTAL APPROACH

Rats received 0, 0.17 or 0.86 mg·kg^{-1} of the D_2 agonist quinpirole i.v. Quinpirole concentrations in plasma and brain extracellular fluid ($brain_{ECF}$), as well as plasma concentrations of 13 hormones and neuropeptides, were measured. Experiments were performed at day 1 and repeated after 7-day s.c. drug administration. PK/PD modelling was applied to identify the *in vivo* concentration–effect relations and neuroendocrine dynamics.

KEY RESULTS

The quinpirole pharmacokinetics were adequately described by a two-compartment model with an unbound $brain_{ECF}$-to-plasma concentration ratio of 5. The release of adenocorticotropic hormone (ACTH), growth hormone, prolactin and thyroid-stimulating hormone (TSH) from the pituitary was influenced. Except for ACTH, D_2 receptor expression levels on the pituitary hormone-releasing cells predicted the concentration–effect relationship differences. Baseline levels (ACTH, prolactin, TSH), hormone release (ACTH) and potency (TSH) changed with treatment duration.

CONCLUSIONS AND IMPLICATIONS

The integrated multi-biomarker PK/PD approach revealed a fingerprint reflecting D_2 receptor activation. This forms the conceptual basis for *in vivo* evaluation of on- and off-target CNS drug effects. The effect of treatment duration is highly relevant given the long-term use of D_2 agonists in clinical practice. Further development towards quantitative systems pharmacology models will eventually facilitate mechanistic drug development.

Abbreviations

ACTH, adenocorticotropic hormone; BDNF, brain-derived neurotrophic factor; CRH, corticotrophin-releasing hormone; FSH, follicle-stimulating hormone; GH, growth hormone; LH, luteinizing hormone; OFV, objective function value; PK/PD, pharmacokinetic/pharmacodynamic; RSE, relative standard error; TIDA, tuberoinfundibular dopaminergic; TSH, thyroid-stimulating hormone

DOI:10.1111/bph.14452

Introduction

Besides insufficient information on drug distribution into and within the brain, a main cause of attrition in CNS drug development is the lack of translational pharmacodynamic biomarkers, that is, preclinical biomarkers that are predictive for clinical effect (Hurko and Ryan, 2005; Soares, 2010; de Lange *et al.*, 2017). This enables the mechanistic extrapolation of drug effects from animals to humans (Danhof *et al.*, 2008; de Lange *et al.*, 2017).

It is important that these biomarkers are accessible in humans. This poses a challenge for CNS drug development, given that sampling from the human brain is highly limited. However, the pituitary hormones and peptides of the neuroendocrine system are released upon signals from the CNS, in particular the hypothalamus, providing an opportunity to study central drug effects in plasma. **Dopamine**, for example, is released from the tuberoinfundibular dopaminergic (TIDA) neurons into the median eminence of the pituitary to control the release of **prolactin** from the lactotrophs into plasma (Freeman *et al.*, 2000). It has been shown that dopamine D_2 agonists stimulate the release of dopamine into the median eminence (Eaton *et al.*, 1993; Durham *et al.*, 1997). This principle has been used to evaluate the dopaminergic drug efficacy with prolactin (Movin-Osswald and Hammarlund-Udenaes, 1995; Petty, 1999; Stevens *et al.*, 2012; Petersson *et al.*, 2013; Taneja *et al.*, 2016; van den Brink *et al.*, 2017), including the translation of these effects from rats to humans (Stevens *et al.*, 2012; Petersson *et al.*, 2013).

Realizing that biological systems behave as networks, single biomarker approaches are increasingly replaced by multi-biomarker approaches (van der Greef and Mcburney, 2005; van der Greef *et al.*, 2007). Although prolactin is a sensitive biomarker for dopamine **D_2 receptor** activation, it is also sensitive to **5-HT** and **thyroid-releasing hormone** (TRH; Lyons and Broberger, 2014). A multi-biomarker approach is envisioned to provide a more specific reflection of D_2 receptor activation. Indeed, the dopaminergic system has multiple connections to the neuroendocrine system, including the release of prolactin, **growth hormone (GH)** and **thyroid-stimulating hormone (TSH)** (Tuomisto and Mannisto, 1985; Pivonello *et al.*, 2007). With that, it is important to identify the pharmacokinetic/pharmacodynamic (PK/PD) parameters that can be scaled from animals to humans (Danhof *et al.*, 2008). Moreover, dopaminergic drug effects may change with increasing duration of treatment following sensitization and tolerance, as was shown for D_2 agonists (Tirelli and Jodogne, 1993).

The aim of the current study was, therefore, to characterize both the short-term and longer-term interactions of the dopaminergic system with the neuroendocrine system, in order to obtain a fingerprint biomarker of D_2 receptor activation. The selective $D_{2/3}$ agonist **quinpirole** will be used as a paradigm compound. Here, we present a PK/PD fingerprint of quinpirole with **adenocorticotropic hormone (ACTH)**, GH, prolactin and TSH as neuroendocrine biomarkers.

Methods

Animals, surgery and experiment

Animals. Animal studies are reported in compliance with the ARRIVE guidelines (Kilkenny *et al.*, 2010; McGrath & Lilley, 2015) and were performed in agreement with the Dutch Law of Animal Experimentation and approved by the Animal Ethics Committee in Leiden, the Netherlands (study protocol DEC12247). Male Wistar rats (n = 44) were housed in groups for 6–9 days until surgery (Animal Facilities Gorlaeus Laboratories, Leiden, the Netherlands). Animals were held under standard environmental conditions while artificial daylight was provided from 7:30 AM to 7:30 PM. They had *ad libitum* access to food (Laboratory chow, Special Diets Services, Tecnilab BMI, Someren, the Netherlands) and acidified water.

Surgery. The surgery was performed following previously reported procedures (Westerhout *et al.*, 2012). The rats received 2% isoflurane anaesthesia while undergoing surgery. After induction of the isoflurane, 0.09 mL Buprecare® (AST Farma B.V., Oudewater, the Netherlands) was administered i.m. Cannulas were placed in the femoral artery for serial blood sampling and the femoral vein for drug administration. Probe guides (CMA/12) with dummy probes were implanted in caudate putamen in both hemispheres (1.0 mm anterior, 3.0 mm lateral, 3.4 mm ventral, relative to bregma) and replaced by the probes (CMA/12 Elite – 4 mm) 24 h before the experiment. After the surgery, the animals received 0.15 mL Ampicillan® (Dechra Veterinary Products B.V., Bladel, the Netherlands) and 3 mL 0.9% NaCl s.c. The rats were individually held in Makrolon type 3 cages for 7 days to recover and weighed on a daily basis to evaluate the recovery.

Experiments. The rats were randomly assigned to receive 0 (n = 12), 0.17 $mg \cdot kg^{-1}$ (n = 16) or 0.86 $mg \cdot kg^{-1}$ (n = 16) i.v. quinpirole between 10:45 AM and 11:15 AM on the first day of the experiment. The smaller group size for the control group was chosen, because less variation was expected in the data, that is, there is no inter-individual variation from PK and the resultant PD processes. The statistical non-linear mixed effect analysis (see Data analysis section) is able to handle unbalanced study designs. The microdialysate samples were collected from −200 to 180 min (20-min interval, 1.5 μL min^{-1}, 120 min equilibration time) in polypropylene microvolume inserts (250 μL; Waters, Etten-Leur, the Netherlands) containing an antioxidant mix of 10 μL 0.02 M formic acid/0.04% ascorbic acid in water. Blood samples of 200 μL were collected in heparin-coated Eppendorf tubes at −5, 5, 7.5, 10, 15, 25, 45, 90, 120 and 180 min and centrifuged (1000× g, 10 min, 4°C) to separate the plasma. All samples were stored at −80°C until blinded analysis. After the experiment, the cannulas were filled with a saline–heparin solution (venous) or a PVP-heparin solution (arterial), while a dummy replaced the probes. The rats received their quinpirole dose s.c., until the second experiment on day 8, which was executed as on day 1. After the

experiment, the rats were killed following an overdose of Nembutal®.

Chemical analysis of the samples

Quinpirole analysis in plasma and microdialysate. Quinpirole (Bio-Connect, Huissen, the Netherlands) was analysed using LC tandem MS (LCMS/MS). Calibration standards were prepared in plasma with 0, 5, 10, 20, 50, 100, 200, 400 and 500 ng·mL^{-1} and in buffered perfusion fluid (bPF) with 0, 0.5, 1, 2, 5, 10, 20, 50, 100 and 200 ng·mL^{-1} quinpirole. Quality controls were prepared in plasma with 5, 10, 50 and 500 ng·mL^{-1} and in bPF with 1, 6, 30 and 150 ng·mL^{-1} quinpirole. Of the microdialysate samples, 20 μL was transferred to microvolume inserts (BGB Analytik, Harderwijk, the Netherlands) and spiked with 20 μL of 40 ng·mL^{-1} internal standard ropinirole-D4 (Bio-Connect). Of the plasma samples, 20 μL was spiked with 20 μL of the same internal standard and 20 μL water before deproteination with 1 mL acetonitrile (AcN). After centrifuging (20 000× *g*, 10 min), the supernatant was transferred to an Eppendorf vial and dried by CentriVap vacuum centrifugation (Labconco, Kansas City, Missouri, USA). The residue was dissolved in 40 μL 5% AcN. After being centrifuged (20 000× *g*, 10 min), the supernatant was transferred to microvolume inserts and inserted into 1.5 mL screw cap vials.

The vials were placed into the Nexera X2 UHPLC–MS/MS system (Shimadzu's Hertogenbosch, the Netherlands) at 10°C; 5 μL of the sample was injected into the system, operated by LCQuan software (version 2.7, Thermo Fisher Scientific, Breda, the Netherlands) and the MS Finnigan TSQ quantum ultra-mass spectrometer (Thermo Fisher Scientific), operated by XCalibur software (version 2.5, Thermo Fisher Scientific). An Acquity UPLC BEH C18 column (130 Å, 1.7 μm, 2.1 mm × 50 mm; Waters) was used with a flow rate of 0.4 mL·min^{-1} and a column temperature of 40°C. The mobile phases were prepared in 10 mM ammonium acetate in water (adjusted to pH 7 with formic acid). The aqueous mobile phase (MP_{AQ}) contained 5% and the organic mobile phase (MP_{ORG}) 95% AcN. A gradient was applied with 10% MP_{ORG} (0–0.5 min) to 100% MP_{ORG} (0.5–2.0 min) and kept at 100% MP_{ORG} (2.0–2.8 min), after which the column was re-equilibrated with 10% MP_{ORG} (2.8–3.0 min). The retention time of quinpirole and ropinirole-D4 was 1.8 and 2.24 min respectively. The MS was used in positive electrospray ionization mode, and all compounds were monitored by selective reaction monitoring. The ionization voltage, capillary energy, capillary temperature and desolvation temperature were set to 3.50 kV, 3 V, 150°C and 400°C respectively. The transition ion pair was 220.18 m/z → 161.00 m/z, 16 V for quinpirole and 265.22 m/z → 132.07 m/z, 32 V for ropinirole-D4. The quality of the method was assured following the guidelines for bioanalysis (Viswanathan *et al.*, 2007). The unbound fraction of quinpirole in plasma was determined to be 71 ± 3% (concentration-independent) by filtrating plasma samples using high-speed filtration (Centrifree®, Merck Millipore, Amsterdam, the Netherlands; 2000× *g*, 10 min) and calculating the ratio of unbound to total plasma concentrations. The total plasma concentrations of quinpirole measured were corrected accordingly to obtain unbound plasma concentrations. The recovery of quinpirole over the microdialysis probe was determined to be 5.4 ± 1.7% (n = 191) using the retrodialysis method (de Lange, 2013). The microdialysate quinpirole concentrations measured were corrected for probe recovery to obtain the $brain_{ECF}$ concentrations.

Pituitary hormones and neuropeptides in plasma. The pituitary hormones [ACTH, **brain-derived neurotrophic factor (BDNF)**, **follicle-stimulating hormone (FSH)**, GH, **luteinizing hormone (LH)**, prolactin and TSH] and neuropeptides (**α-melanocyte-stimulating hormone**, **β-endorphin**, **neurotensin**, **orexin A**, **oxytocin**, **substance P**) were analysed by multiplex assays (RTPMAG-86K and RMNPMAG-83K, Merck Millipore, Darmstadt, Germany) on a Bio-Plex® MAGPIX™ system (BioRad Laboratories, Veenendaal, the Netherlands). With the RTPMAG-86K, 10 μL and with the RMNPMAG-83K, 50 μL plasma was used for analysis according to the protocol provided by the manufacturer.

Data analysis

The data and statistical analysis comply with the recommendations on experimental design and analysis in pharmacology (Curtis *et al.*, 2018).

PK/PD modelling software and criteria. The PK/PD models to describe the quinpirole and the hormone concentrations in $brain_{ECF}$ and plasma were developed by a two-stage approach (the PK parameters were fixed before developing the PD models), using a non-linear mixed effect population approach in NONMEM® version 7.3.0 with subroutine ADVAN13. The inter-individual variability around the parameters and the residual error was described by an exponential distribution (Supporting Information Equations S1 and S2). Model selection was based on successful convergence, objective function value (OFV), parameter precision and visual evaluation of the model predictions as compared to the observations.

Pharmacokinetic model development. Two- and three-compartment models were compared, with both linear or non-linear clearance from plasma for their description of unbound quinpirole concentrations in plasma and $brain_{ECF}$. Here, it should be noted that a two-compartment model refers to one compartment describing plasma and another compartment describing $brain_{ECF}$ quinpirole concentrations. The transport into and out of the brain across the blood–brain-barrier in these models was estimated with two separate distribution clearances. The experiment day was evaluated as covariate on one of the model parameters. The model selected was evaluated on additional data to guarantee external validity, and the details of which are described in the Supporting Information Data S1.

Pharmacodynamic model development. For each hormone, baseline, PK/PD and covariate models were developed in a step-wise manner. Baseline patterns were evaluated on placebo data following Supporting Information Equations S4–S7, Part I. The selected baseline models were, together with the pharmacokinetic model, integrated into the PK/PD models. The PK/PD models were defined as a combination of the following characteristics: (i) baseline model for each

hormone, (ii) plasma or $brain_{ECF}$ as target site, (iii) the slope, the E_{MAX}, the alternative E_{MAX} (Schoemaker *et al.*, 1998), the on–off or no drug effect model, and (iv) the direct response, the turnover or the pool model as link model (Supporting Information Equations S9–S16, Part I). The best model was automatically selected on the basis of model convergence and OFV. Finally, the PK/PD models selected were evaluated for an effect of experiment day using step-wise covariate model building (Khandelwal *et al.*, 2011) (Supporting Information Equations S17–S19, Part I).

Estimation of signal transduction efficiency. The quantitative relation between receptor binding and pharmacological effect depends on the signal transduction efficiency (Jonker *et al.*, 2005; Danhof *et al.*, 2007), which is made explicit in the operational model of agonism (Black and Leff, 1983). Therefore, the PK/PD models selected were simulated and fitted by the operational model (Equation 1) (Black and Leff, 1983; Danhof *et al.*, 2007):

$$E = \frac{E_m * \tau * C}{k_A + (1+\tau) * C}. \quad (1)$$

In which E_m is the systems maximum, τ is the transduction efficiency and k_A is the affinity for the D_2 receptor. It was assumed that the target site of action is in the $brain_{ECF}$. Furthermore, the assumption was made that quinpirole is selective for the dopamine D_2 receptor, and the GH, prolactin and TSH responses were modulated *via* the TIDA neurons (Figure 2). Therefore, the affinity of quinpirole to the D_2 receptor was estimated equal among all hormones, while the signal transduction efficiency of GH, prolactin and TSH was assumed dependent on pituitary D_2 receptor expression obtained from literature (Goldsmith *et al.*, 1979). The D_2 receptor expression for somatotrophs, lactotrophs and thyrotrophs was calculated as the number of 'troph' cells expressing the D_2 receptor relative to the total number of 'troph' cells. This relation to the signal transduction efficiency was made explicit following Equation 2:

$$\tau = \tau_0 * e^{slp * receptor\ expression}, \quad (2)$$

where τ is estimated for GH, prolactin and TSH on the basis of the pituitary D_2 receptor expression.

Nomenclature of targets and ligands

Key protein targets and ligands in this article are hyperlinked to corresponding entries in http://www.guidetopharmacology.org, the common portal for data from the IUPHAR/BPS Guide to PHARMACOLOGY (Harding *et al.*, 2018), and are permanently archived in the Concise Guide to PHARMACOLOGY 2017/18 (Alexander *et al.*, 2017).

Results

Pharmacokinetics of quinpirole in plasma and $brain_{ECF}$

A two-compartment model best described the pharmacokinetics of quinpirole in plasma and $brain_{ECF}$ with linear first-order elimination from plasma and a net active influx from plasma to $brain_{ECF}$ (Supporting Information Equation S3). The parameter estimates were precise and accurate (Table 1), and the model could well describe the quinpirole concentrations in plasma and $brain_{ECF}$ over a large dose range (Figure 1A). Although there is a slight over-prediction of quinpirole concentrations in $brain_{ECF}$, external validation showed good extrapolative ability of the model (Figure 1B).

Responding pituitary hormones and neuropeptides in plasma. On the basis of automated model selection, the hormones luteinizing hormone, prolactin and TSH showed a placebo response described by circadian rhythm with a

Table 1

Parameter estimates of the quinpirole pharmacokinetic model

	Model evaluation		Bootstrap (n_{btstr} = 168)	
Parameter	**Estimate**	**(RSE)[shr]**	**Estimate**	**(CV)**
$CL_{PL,o}$ ($L \cdot h^{-1}$)	0.71	(9%)	0.70	(9%)
IIV $CL_{PL,o}$	0.12	(32%) [7%]	0.12	(35%)
$CL_{PL,ECF}$ ($L \cdot h^{-1}$)	2.5	(20%)	2.5	(19%)
$CL_{ECF,PLASMA}$ ($L \cdot h^{-1}$)	0.52	(24%)	0.55	(24%)
$k_{p,uu}$ ($CL_{PL,ECF}/CL_{ECF,PL}$)	5	–	–	–
$V_{CENTRAL}$ (L)	1.0	(6%)	1.0	(7%)
V_{ECF} (L)	0.12	(13%)	0.013	(17%)
RUV $C_{QP,PL}$	0.08	(24%) [3%]	0.08	(24%)
RUV $C_{QP,ECF}$	0.12	(28%) [2%]	0.12	(30%)

C, concentration; CL, clearance; CV, coefficient of variation; ECF, brain extracellular fluid; IIV, inter-individual variability; $k_{p,uu}$, ratio of unbound $brain_{ECF}$ and plasma drug concentration; n_{btstr}: number of successful bootstrap model runs out of a total of 200 runs; PL, plasma; RUV, residual unexplained variability; shr, shrinkage; V, volume of distribution.

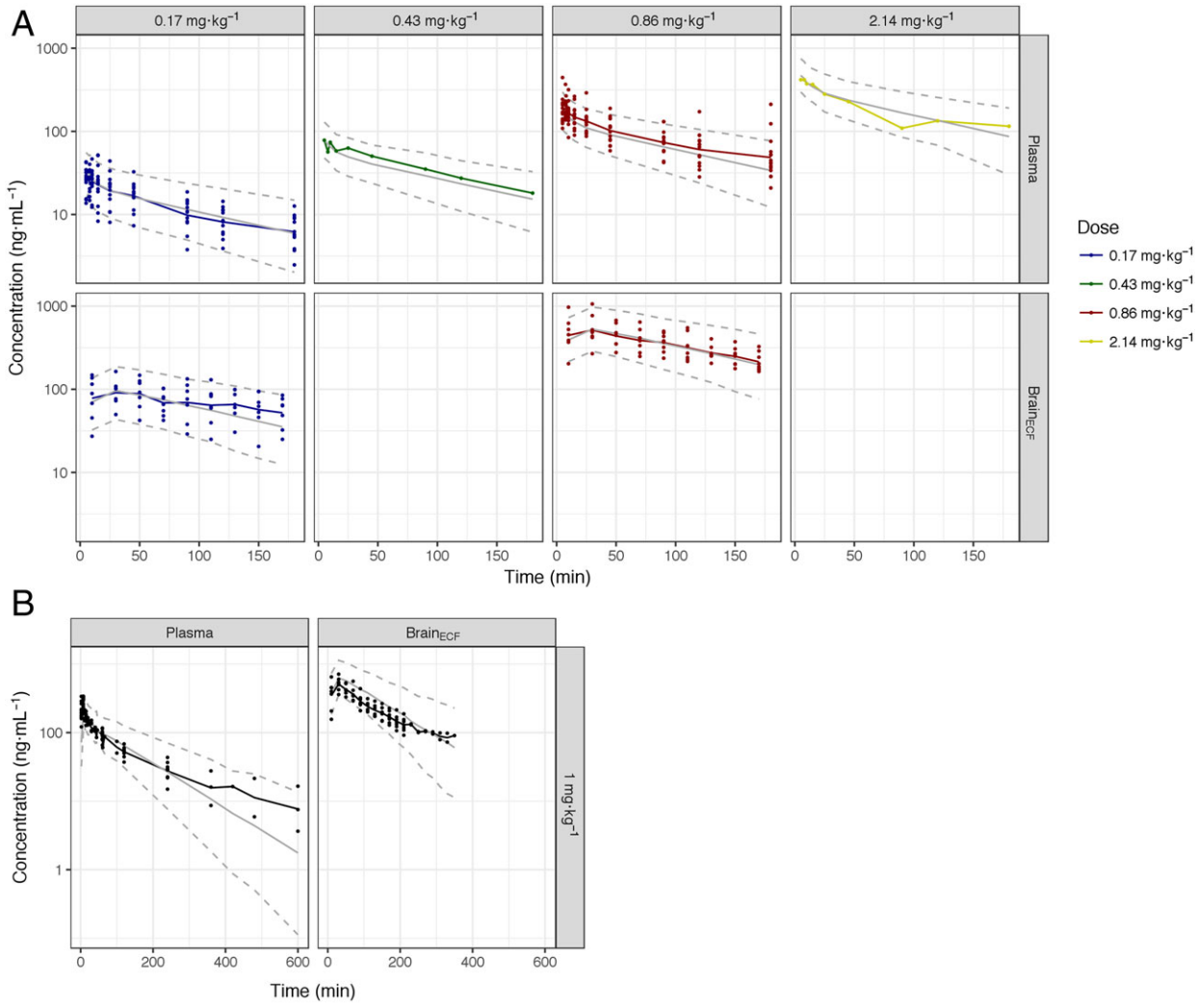

Figure 1

Visual predictive check (A) and external validation (B) for the quinpirole pharmacokinetic model in plasma and brain$_{ECF}$. The coloured dots represent the observed data, with the solid coloured lines showing the mean of the observations. The solid grey line shows the mean, and the dashed grey lines show the 90% confidence interval of 500 simulations. *The experiments in which the animals received 0.43 mg·kg^{-1} and 2.14 mg·kg^{-1} represented experimental protocol deviations (higher dose) and were included in PK model development only.

period of 120 min, the Bateman equation or exponential decay respectively (Supporting Information Figure S1A). A model with no baseline pattern best described the other hormone baselines. ACTH, GH, prolactin and TSH responded to quinpirole treatment with diverse PK/PD relations, while no effect was observed on the neuropeptides, BDNF, FSH and LH, following automated model selection (Supporting Information Figure S1B, Table 2). Except for $k_{deg,ACTH}$ [relative standard error (RSE) = 282%] and $EC_{50,Prl}$ (RSE = 99%), the parameters were identified with reasonable precision (Table 3), and the models could describe the data well (Supporting Information Equations, Part II; Figure S2).

Target site of effect. No statistically significant difference was identified comparing the best models for ACTH, GH, prolactin and TSH with either plasma or brain$_{ECF}$ as target site (Table 3).

Mechanistic evaluation of quinpirole effect on ACTH, GH, prolactin and TSH. The concentration–effect relations between quinpirole and every single hormone are depicted in Figure 3, assuming brain$_{ECF}$ as target site (Table 3). Prolactin was most sensitive to quinpirole with a potency of 0.93 ng·mL^{-1}, while ACTH, GH and TSH responded with a potency of 54 ng·mL^{-1}, 101 ng·mL^{-1} and 178 ng·mL^{-1} respectively (Table 3). The operational model could fit the simulated concentration–effect relationships well (Figure 3; Table 4). Within this model, the signal transduction efficiency values (τ) of GH, prolactin and TSH could be related to the pituitary receptor expression on the somatotrophs, lactotrophs and thyrotrophs respectively. In contrast, the ACTH concentration–response relationship could not be fitted under the assumption of signal transduction efficiency being dependent on pituitary D_2 receptor expression (Supporting Information Figure S3).

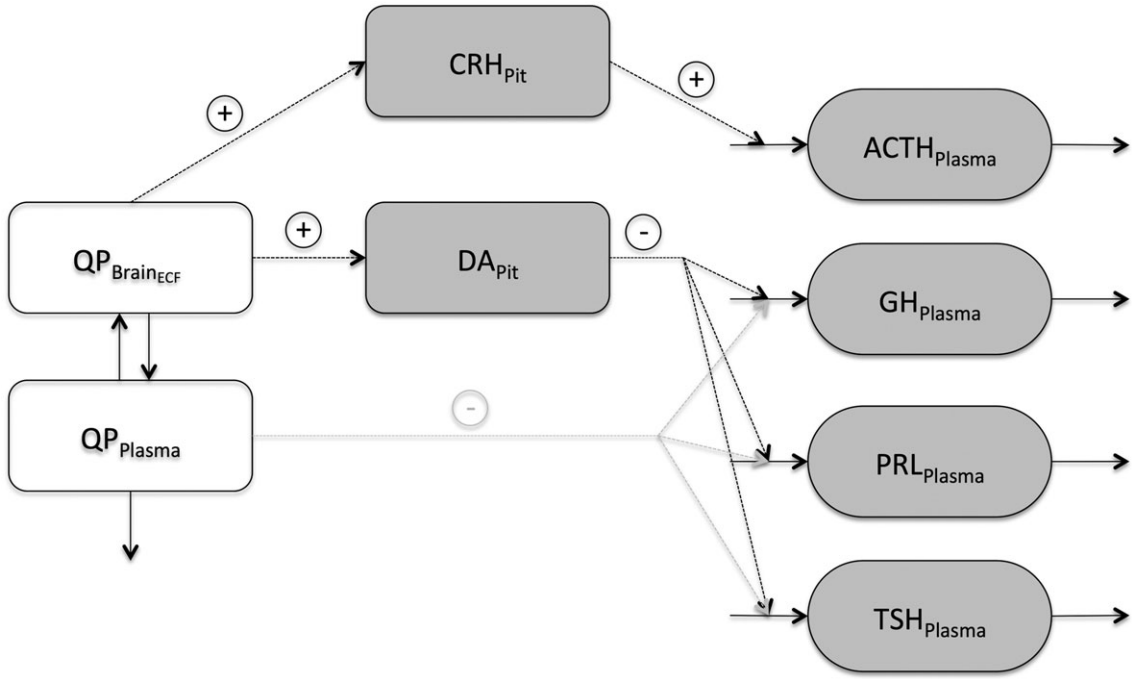

Figure 2

The interaction between quinpirole and the neuroendocrine system with the pharmacokinetics as white compartments and the pharmacodynamics as grey compartments. Quinpirole stimulates TIDA neurons in the hypothalamus to increase the release of dopamine into the pituitary. Dopamine inhibits the release of GH, prolactin (PRL) and TSH into plasma. ACTH was stimulated by quinpirole, suggesting a pathway other than TIDA neuron stimulation. The site of the main effect is assumed to be the brain, given the high quinpirole in $brain_{ECF}$ as compared to plasma. QP, quinpirole; DA, dopamine.

Table 2

The PK/PD effects of quinpirole on ACTH, GH, prolactin and TSH, including the PK/PD model type and target site of drug action that was identified

Hormone	Effect	PK/PD model	Target site
ACTH	+	Slope model and pool model with stimulation of k_{REL}	Plasma
GH	−	E_{MAX} model and turnover model with inhibition of k_{REL}	$Brain_{ECF}$
Prolactin	−	E_{MAX} model and turnover model with inhibition of k_{REL}	$Brain_{ECF}$
TSH	−	E_{MAX} model and turnover model with inhibition of k_{REL}	$Brain_{ECF}$

ECF, extracellular fluid; Effect: + increased release, − reduced release; k_{REL}, hormone release rate.

One-day versus eight-day treatment responses. The pharmacokinetics of quinpirole were not significantly influenced by 8-day drug treatment. In contrast, the pharmacodynamics showed a significant change for ACTH, prolactin and TSH (Supporting Information Table S1). The differences between the responses after short- and long-term treatment are graphically presented in Figure 4. The basal levels of ACTH were increased independent of dose, while the hormone release rate was increased in a dose-dependent manner. This resulted in a lower maximal ACTH response after 8-day treatment with a high dose as compared to a low dose of quinpirole. The basal prolactin concentrations after 8 days were increased with dose, while the extent of the placebo effect was decreased, independent of dose. The basal levels of TSH have decreased with 8-day treatment regardless the dose, while the sensitivity to quinpirole (EC_{50}) was decreased in a dose-dependent manner.

Discussion

This study systematically evaluated the effects of quinpirole on the neuroendocrine system following a PK/PD based multi-biomarker approach. Quinpirole showed a high rate of transport over the blood–brain-barrier with an unbound partition coefficient ($k_{p,uu}$) of 5. ACTH, GH, prolactin and TSH responded to quinpirole, each with a unique target site

Table 3

Parameter estimates of the PK/PD models for quinpirole effect on ACTH, GH, prolactin and TSH with plasma and $brain_{ECF}$ as target site

	Plasma Estimate (RSE)	$Brain_{ECF}$ Estimate (RSE)
ACTH		
OFV	−31.3	−32.9
Baseline ($pg \cdot mL^{-1}$)	3.74 (17%)	3.71 (17%)
$IIV_{Baseline}$	0.68 (71%) [0%]	0.68 (72%) [0%]
Slope ([$ng \cdot mL^{-1}$])	0.873 (43%)	–
E_{MAX}	–	2.35 (11%)
EC_{50} ($ng \cdot mL^{-1}$)	–	54.1 (40%)
K_{DEG} (min^{-1})	0.0146 (24%)	308 (282%)
K_{REL} (min^{-1})	0.00760 (29%)	0.00421 (31%)
RUV	0.27 (21%) [3%]	0.27 (21%) [3%]
GH		
OFV	667.6	664.1
Baseline ($pg \cdot mL^{-1}$)	1002 (n.a.)	992 (25%)
E_{MAX}	−1 (n.a.)	−1 (39%)
S_0 ([$ng \cdot mL^{-1}$])	0.0545 (n.a.)	0.00985 (53%)
EC_{50} ($ng \cdot mL^{-1}$)	18.4 (calc.)	101 (calc.)
K_{DEG} (min^{-1})	0.0228 (n.a.)	0.0282 (22%)
RUV	2.48 (13%)	2.45 (13%)
Prolactin		
OFV	377.0	373.5
Baseline ($pg \cdot mL^{-1}$)	284 (25%)	262 (25%)
$IIV_{Baseline}$	0.70 (28%) [4%]	0.67 (28%) [4%]
D_{Plac} ($pg \cdot mL^{-1}$)	8.72 (fix)	8.72 (fix)
$K_{IN,\ Plac}$ (min^{-1})	1.65 (fix)	1.65 (fix)
$K_{DEC,\ Plac}$ (min^{-1})	1.55 (fix)	1.55 (fix)
E_{MAX}	−0.961 (21%)	−0.959 (13%)
EC_{50} ($ng \cdot mL^{-1}$)	0.0983 (275%)	0.933 (99%)
K_{DEG} (min^{-1})	0.584 (22%)	0.0652 (22%)
RUV	0.79 (18%) [3%]	0.79 (18%) [3%]
TSH		
OFV	−272.2	−270.0
Baseline ($pg \cdot mL^{-1}$)	305 (5.3%)	293 (4.7%)
$IIV_{Baseline}$	0.047 (30%) [8%]	0.045 (30%) [9%]
$K_{DEC,\ Plac}$ (min^{-1})	0.00489 (fix)	0.00489 (fix)
E_{MAX}	−0.819 (36%)	−0.794 (32%)
EC_{50} (ng/mL)	31.2 (30%)	178 (34%)
K_{DEG} (min^{-1})	0.0781 (13%)	0.126 (20%)
RUV	0.17 (19%) [2%]	0.18 (19%) [2%]

In bold the parameters of the selected models. D_{Plac}, the extent of the placebo effect; ECF, extracellular fluid; EC_{50}, concentration at half maximal drug effect; E_{MAX}, maximal drug effect; k_{DEC}, dose-independent hormone decay; k_{DEG}, hormone elimination rate; k_{REL}, hormone release reate; RUV, residual unexplained variability; S_0, E_{MAX}/EC_{50}.

concentration–effect relationship, providing a fingerprint of D_2 receptor activation. Additionally, while no changes were found in PK, the pharmacodynamics changed with 8-day

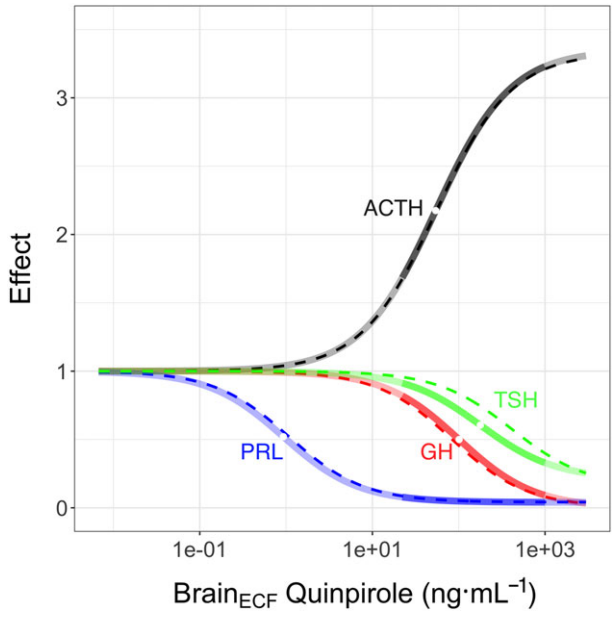

Figure 3

(A) Simulated concentration–effect relationships for ACTH, TSH, GH and prolactin (PRL) on the basis of the parameter estimates in Table-3. The dark segments represent the quinpirole concentration range measured in $brain_{ECF}$. The dotted lines represent the fit with the operational model, in which the signal transduction efficiency τ for GH, prolactin and TSH is dependent on D_2 receptor expression following Equation 2.

Table 4

Relative D_2 receptor expression on the troph cells in the rat anterior pituitary, the signal transduction efficiency τ and the systems maximal effect E_m estimated from the operational model in Equation 1

	D_2 receptor expression (Goldsmith *et al.*, 1979)	τ	E_M
Corticotrophs (ACTH)	20%	13.8	2.51
Somatotrophs (GH)	34%	8.7	−1.11
Lactotrophs (prolactin)	76%	743	−0.96
Thyrotrophs (TSH)	13%	0.94	−1.76

The k_A was estimated 805 $ng \cdot mL^{-1}$ (see Equation 1), while the τ_{GH}, $\tau_{prolactin}$, τ_{TSH} was described by $\tau = 0.24 * e^{0106 * receptor\ expression}$.

administration both dependent and independent of the quinpirole dose. This study underlines the need for integrative multi-biomarker evaluations of drug effects to comprehend the system-wide pharmacological profile.

Can the target site of effect be determined?

Since the ultimate purpose is to identify peripheral biomarkers of the central drug effect, an important question is

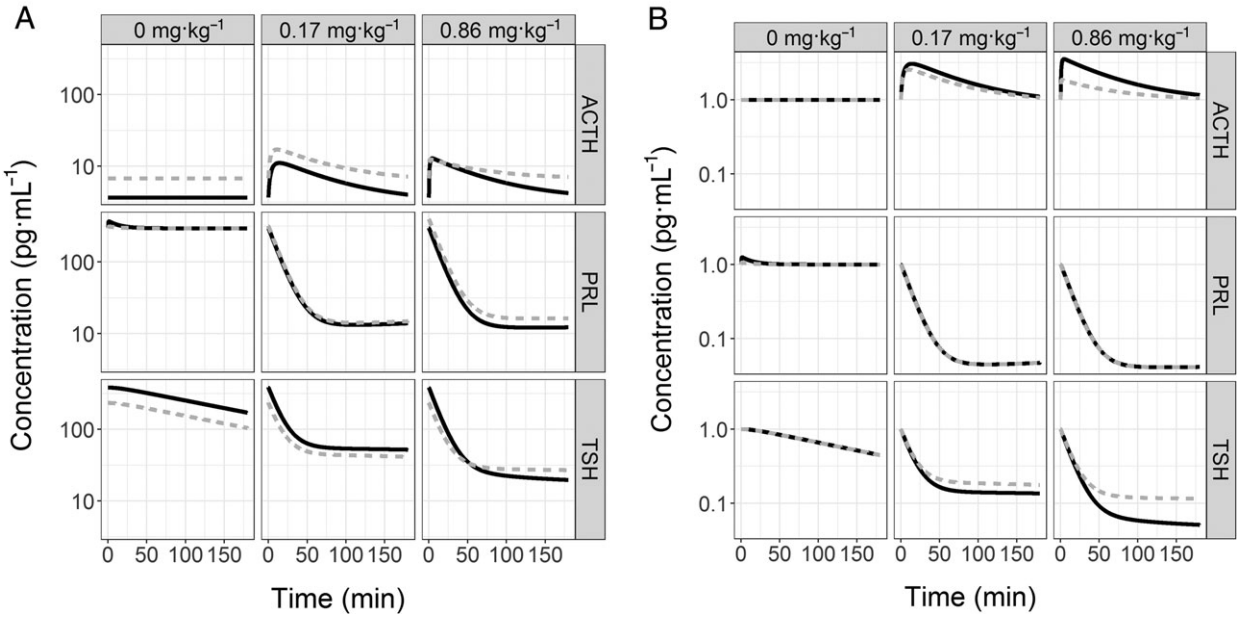

Figure 4

Simulated hormone actual (A) and baseline normalized (B) concentration-time profiles of ACTH, prolactin (PRL) and TSH after one administration (solid black line) and eight administrations (dashed grey line).

whether we can consider $brain_{ECF}$ concentrations as the target site concentrations of the effect of quinpirole. We have shown that, on the basis of statistical significance, it was not possible to discriminate between $brain_{ECF}$ and plasma as target site of effect. Given that the D_2 receptors on the 'troph' cells are accessible from plasma and the release of these hormones have been modified by systemic dopamine infusion (Besses *et al.*, 1975; Vance *et al.*, 1987), it is suggested that these hormones are released upon peripheral drug action. On the other hand, the release of these hormones is tightly controlled by signals from the hypothalamus that are highly connected to dopamine and other neurotransmitter systems. Considering this, the rate and extent of drug distribution into the brain may determine the dominant target site of effect. For the D_2 antagonist remoxipride ($k_{p,uu}$ = 1) (van den Brink *et al.*, 2017), $brain_{ECF}$ could be considered as target site to release prolactin into plasma, while for the D_2 antagonist risperidone ($k_{p,uu}$ = 0.45) (Yamamoto *et al.*, 2016), plasma could be considered as target site (Stevens *et al.*, 2012; Shimizu *et al.*, 2017; van den Brink *et al.*, 2017). Quinpirole is found to be subjected to active influx: although no information on the transporter is available in literature, it is observed that, under steady state conditions, the free drug concentration in $brain_{ECF}$ is as much as five times higher than in plasma ($k_{p,uu}$ = 5; Table 1). Therefore, although we could not provide a statistical determination, it is presumed that the main effect of quinpirole on the neuroendocrine system is mediated *via* the brain rather than *via* the periphery.

Interpretation of the unique concentration–effect relationships

Dopamine activity in the brain is reflected in the tuberoinfundibular dopamine pathway that consists of three types of neurons that project from the hypothalamus to the pituitary: (i) the TIDA neurons, (ii) the periventricular hypophyseal dopamine neurons and (iii) the tuberohypophyseal dopamine neurons (Freeman *et al.*, 2000). TIDA neurons release dopamine into the long portal veins of the pituitary to which the 'troph' cells are exposed. While quinpirole has affinity for both the D_2 and the **D_3 receptor** (Millan *et al.*, 2002), the effects on the neuroendocrine system are putatively mediated *via* the D_2 receptor because of the following findings. First, the enhancing effect of quinpirole on ACTH release was reversed with administration of the D_2 receptor antagonist sulpiride (Borowsky and Kuhn, 1992; Kurashima *et al.*, 1996). Second, the effect of quinelorane, which is similarly specific for the $D_{2/3}$ receptor, on the neuroendocrine TIDA neurons was antagonized by the selective D_2 receptor antagonist raclopride (Eaton *et al.*, 1993). Third, while the selective D_2 agonist PNU-95666 activated the TIDA neurons and inhibited prolactin release, this was not the case for the selective D_3 agonist PD128907 (Durham *et al.*, 1997). In contrast, studies with selective D_2 and D_3 agonists in ovariectomized oestrogen-primed female rats showed a decrease of TIDA neuron activity and an increase of subsequent prolactin release (Liang and Pan, 2012; Liang *et al.*, 2014). However, the oestrogen-priming in these studies prevents a direct comparison between these results and our results, since oestrogen interferes with TIDA neuron activity as well as the sensitivity of the pituitary to dopamine (Gudelsky *et al.*, 1981; Morel *et al.*, 2009). Indeed, our study design is more similar to that of the studies observing activation of TIDA neuron activity and suppression of prolactin release, that is, they studied male rats or diestrous female rats with low oestrogen levels (Eaton *et al.*, 1993; Durham *et al.*, 1997). Therefore, we assume that the stimulation of TIDA neuron activity by of quinpirole in our

study is D_2 specific. Dopamine D_2 receptors were identified not only on lactotrophs (prolactin) but also on corticotrophs (ACTH), somatotrophs (GH), gonadotrophs (FSH, LH) and thyrotrophs (TSH) (Goldsmith *et al.*, 1979; Pivonello *et al.*, 2007). Also, dopamine agonists inhibited the release of ACTH, GH, prolactin and TSH *in vitro*, likely mediated *via* the D_2 receptors (Ishibashi and Yamaji, 1984, 1981; Foord *et al.*, 1986). Overall, it is thus expected that ACTH, GH, prolactin and TSH concentrations decrease with quinpirole treatment upon the stimulation of TIDA neuron activity that enhances dopamine release into the pituitary to bind to the pituitary dopamine receptors on the 'troph' cells. Interestingly, the secretion of ACTH was increased, indicating a different mechanism of action not *via* the TIDA neurons. The hypothalamic mediator of ACTH release is corticotrophin-releasing hormone (CRH). CRH is under control of several neurotransmitters, for example, noradrenaline and γ-aminobutyric acid. Since the effect of quinpirole on ACTH was found to be D_2 receptor specific (Borowsky and Kuhn, 1992), it is likely that CRH or the controlling neurotransmitters are influenced in a D_2 specific manner (Figure 2).

According to these mechanisms, the assumptions of D_2 receptor selectivity for all hormones and the pituitary D_2 receptor expression dependent signal transduction for GH, prolactin and TSH were made (Figure 2; Table 4). Conceptually, the differences in signal transduction efficiency may also be explained by differences in fractional receptor occupancy needed to elicit a certain level of pituitary hormone release, that is, the release of some hormones may be more sensitive to dopamine receptor activation than to that of other hormones. However, our assumptions are confirmed by a good fit of the operational model on the simulated concentration effect relationships as depicted in Figure 3. Physiologically, this suggests a receptor expression dependent sensitivity of the hormones to the increase of pituitary dopamine following the central quinpirole effect. In fact, it indicates that τ indeed is a system-specific parameter. The opposed direction of the ACTH response and the deviation of τ_{ACTH} from the relation between receptor expression and τ indicate a different mechanism of action of D_2 receptor activation on ACTH release (Figure 3; Table 4; Supporting Information Figure S3). Altogether, the systems response expressed in terms of signal transduction efficiency provides a fingerprint that is specific for D_2 receptor stimulation in the brain.

Habituation, tolerance and homeostatic feedback mechanisms

There are three mechanisms through which the differences between day 1 and day 8 are explained (Figure 4). First of all, the dose-independent changes are likely the consequence of habituation; the animals' response to the daily injection procedure returns to basal levels with longer term administration. Indeed, the ACTH and TSH basal levels and the prolactin placebo response changed over the period of quinpirole administration (Figure 4). Second of all, pharmacodynamic tolerance may occur as a consequence of long-term drug administration (Dumas and Pollack, 2008). Tolerance is the mechanism of physiological adaptation to continuous external stimuli, for example, the change in receptor expression. Pharmacodynamic tolerance was identified for the TSH response, as indicated by the dose-dependent change of EC_{50} (Figure 4, Supporting Information Table S1). Assuming a D_2-dependent mechanism, this cannot be explained by reduced hypothalamic D_2 receptor expression, since this was not observed for the other hormones. Moreover, D_2 receptor expression was found not to change with long-term D_2 agonist exposure (Cho *et al.*, 2010). Possibly, the balance between other mediators of TSH release and dopamine has changed, thereby influencing the transduction efficiency. Third of all, the differences between the experiment days can be explained by homeostatic feedback mechanisms. The release rates of ACTH and prolactin were increased in a dose-dependent manner, suggesting a positive and negative feedback respectively (Figure 4; Supporting Information Table S1). These hormones are components of highly complex networks that include multiple negative and positive feedback mechanisms that are affected by 8-day administration of quinpirole. The net effect is reflected in the current analysis, showing that these networks have changed to another equilibrium.

Strengths, limitations and future research

Our integrated PK/PD approach included multiple hormones and neuropeptides that provide comprehensive insight into the interaction between quinpirole and the neuroendocrine system to reveal a fingerprint reflecting D_2 receptor activation. Nevertheless, it has a few limitations that will be discussed in this section. First of all, the 3-h duration of the experiments limited the evaluation of the full pharmacodynamic response. While ACTH levels were back to baseline at the end of the experiment, GH, prolactin and TSH levels were still decreased. This may have limited the precise identification of the PK/PD model, although, in general, the parameter estimates showed good precision. Second, while for ACTH, prolactin and TSH the baseline pattern could be well described; this appeared more difficult for GH. Visual evaluation of the baseline GH pattern indicates that there might be temporal variation. However, no statistically significant or robust model could be identified describing such pattern. High random variation in the data may have prevented such identification. Larger sample sizes than used in the current study are advised to include the possible temporal variation of GH. Third, a wider dose range may have enabled better identification of the EC_{50} parameter in case of, for example, ACTH that was best described by a slope model. However, since a relatively untargeted approach was applied, it was not possible to anticipate the dose range beforehand. Moreover, the current choice of doses was based on an experimental regimen, reflecting the therapeutic range (Gao *et al.*, 1998; Adachi *et al.*, 2003), in order to gain pharmacologically relevant insights. Fourth, the choice of hormones and neuropeptides, although guided by pharmacological knowledge, was based on the available platforms rather than based on the physiology. While this provides a non-biased evaluation of neuroendocrine effects of quinpirole, there is a series of hormones that will be of interest for further research, for example, the downstream signals of the pituitary hormones, such as will be discussed below.

Suggestions for further investigation include the validation of the D_2 receptor activation fingerprint with other

selective D_2 agonists, for example, quinelorane and ropinirole (Millan *et al.*, 2002). Furthermore, we suggest efforts towards unravelling the mechanisms underlying the quinpirole–hormone relationships that were identified in the current study. Such investigation should include (i) the measurement of quinpirole and dopamine in the hypothalamus using microdialysis (Li and Yan, 2010); (ii) the measurement of quinpirole and CRH, GHRH, dopamine and TRH in the pituitary using microdialysis (Granveau-Renouf *et al.*, 2000); (iii) the measurement of ACTH, GH, prolactin and TSH in plasma; (iv) the measurement of corticosterone, IGF-1, triiodithyronine, thyroxine as downstream signals of ACTH, GH and TSH respectively; and (v) a study duration of at least 6 h of experiment. This takes into account the duration of quinpirole exposure (~4 h) as well as the delay of the hormone responses.

Such data will form the basis of a quantitative systems pharmacology model describing the interaction between quinpirole and neuroendocrine system in terms of purely drug- and system-specific parameters. This will also allow the separation of central and peripheral quinpirole effect since the drug concentration will be evaluated in both the hypothalamus and the pituitary. Moreover, the upstream hormones that are released from the hypothalamus will exclusively reflect the hypothalamic interaction with the drug. Eventually, such model can be evaluated with different lengths of chronic administration periods to mechanistically understand the tolerance and homeostatic feedback mechanisms.

Conclusion

The current study has made the case for an integrated and system-wide approach to understand the interaction between dopaminergic pharmacology and the neuroendocrine system. It was shown that, under standard experimental conditions, quinpirole interferes with the hypothalamus–pituitary–adrenal axis (ACTH), the growth hormone system (GH), parts of the reproductive system (prolactin) and the thyroid function (TSH). With this multi-biomarker approach, a fingerprint of transduction efficiency values was obtained that is specific for D_2 receptor activation. In contrast to prolactin alone, as a classical biomarker, this multi-biomarker fingerprint provides a specific reflection of D_2 receptor activation. Our study also indicated a clear change of the PK/PD relationship with comparing short-term and long-term administration. This is highly relevant, considering the long-term use of D_2 receptor agonists in clinical practice. Further understanding of the underlying tolerance and homeostatic feedback mechanisms will increase the proper application of these drugs in clinical practice.

In conclusion, this study provided further insights into the interaction between dopaminergic pharmacology and the neuroendocrine system. Using a multi-biomarker approach, a fingerprint of D_2 receptor activation was obtained. This forms the conceptual basis for the *in vivo* evaluation of the on- and off-target effects of drugs in the CNS. Further efforts towards quantitative systems pharmacology model development will eventually lead to mechanistic translational dopaminergic drug development.

Acknowledgements

We would like to thank Fred Koddekee and Anouk Koot for their assistance with the s.c. injections and Michiel van Esdonk for his help in automating the model evaluation process.

Author contributions

W.B., R.H., Y.W., P.G. and E.L. contributed to the study design. W.B., D.B., F.B., R.H. and Y.W. contributed to the acquisition of data. W.B. performed the analysis of the data. W.B., Y.W., P.G. and E.L. contributed to the writing of the manuscript.

Conflict of interest

The authors declare no conflicts of interest.

Declaration of transparency and scientific rigour

This Declaration acknowledges that this paper adheres to the principles for transparent reporting and scientific rigour of preclinical research recommended by funding agencies, publishers and other organisations engaged with supporting research.

References

Adachi K, Hasegawa M, Fujita S, Lee J, Cools AR, Waddington JL *et al.* (2003). Prefrontal, accumbal [shell] and ventral striatal mechanisms in jaw movements and non-cyclase-coupled dopamine D1-like receptors. Eur J Pharmacol 473: 47–54.

Alexander SPH, Christopoulos A, Davenport AP, Kelly E, Marrion NV, Peters JA *et al.* (2017). The Concise Guide to PHARMACOLOGY 2017/18: G protein-coupled receptors. Br J Pharmacol 174: S17–S129.

Besses GS, Burrow GN, Spaulding SW, Donabedian RK (1975). Dopamine infusion acutely inhibits the TSH and prolactin response to TRH. J Endocrinol Metab 41: 985–988.

Black JW, Leff P (1983). Operational models of pharmacological agonism. Proc R Soc B Biol Sci 220: 141–162.

Borowsky B, Kuhn CM (1992). D_1 and D_2 dopamine receptors stimulate hypothalamo-pituitary-adrenal activity in rats. Neuropharmacology 31: 671–678.

Cho D, Zheng M, Min C, Ma L, Kurose H, Park JH *et al.* (2010). Agonist-induced endocytosis and receptor phosphorylation mediate resensitization of dopamine D_2 receptors. Mol Endocrinol 24: 574–586.

Curtis MJ, Alexander S, Cirino G, Docherty JR, George CH, Giembycz MA *et al.* (2018). Experimental design and analysis and their reporting II: updated and simplified guidance for authors and peer reviewers. Br J Pharmacol 175: 987–993.

Danhof M, de Jongh J, De Lange ECM, Della Pasqua O, Ploeger BA, Voskuyl RA (2007). Mechanism-based pharmacokinetic-

pharmacodynamic modeling: biophase distribution, receptor theory, and dynamical systems analysis. Annu Rev Pharmacol Toxicol 47: 357–400.

Danhof M, de Lange ECM, Della Pasqua OE, Ploeger BA, Voskuyl RA (2008). Mechanism-based pharmacokinetic-pharmacodynamic (PK-PD) modeling in translational drug research. Trends Pharmacol Sci 29: 186–191.

de Lange, ECM (2013). Recovery and calibration techniques: toward quantitative microdialysis. In: Müller M (ed.). Microdialysis in drug development, Vol. IV. Springer-Verlag: New York, pp. 13–33.

de Lange ECM, van den Brink WJ, Yamamoto Y, de Witte WEA, Wong YC (2017). Novel CNS drug discovery and development approach: model-based integration to predict neuro-pharmacokinetics and pharmacodynamics. Expert Opin Drug Discov 12: 1207–1218.

Dumas EO, Pollack GM (2008). Opioid tolerance development: a pharmacokinetic/pharmacodynamic perspective. AAPS J 10: 537–551.

Durham RA, Eaton MJ, Moore KE, Lookingland KJ (1997). Effects of selective activation of dopamine D_2 and D_3 receptors on prolactin secretion and the activity of tuberoinfundibular dopamine neurons. Eur J Pharmacol 335: 37–42.

Eaton MJ, Gopalan C, Kim E, Lookingland KJ, Moore KE (1993). Comparison of the effects of the dopamine D_2 agonist quinelorane on tuberoinfundibular dopaminergic neuronal activity in male and female rats. Brain Res 629: 53–58.

Foord SM, Peters JR, Dieguez C, Hall R, Scanlon MF (1986). Thyrotropin regulates thyrotroph responsiveness to dopamine in vitro. Endocrinology 118: 1319–1326.

Freeman ME, Kanyicska B, Lerant A, Nagy G (2000). Prolactin: structure, function, and regulation of secretion. Physiol Rev 80: 1523–1631.

Gao W, Lee TH, Ph D, King GR, Ph D, Ellinwood EH (1998). Alterations in baseline activity and quinpirole sensitivity in putative dopamine neurons in the substantia nigra and ventral tegmental area after withdrawal from cocaine pretreatment. Neuropsychopharmacology 18: 222–232.

Goldsmith PC, Cronin MJ, Weiner RI (1979). Dopamine receptor sites in the anterior pituitary. J Histochem Cytochem 27: 1205–1207.

Granveau-Renouf S, Valente D, Durocher A, Grognet J-M, Ezan E (2000). Microdialysis study of bromocriptine and its metabolites in rat pituitary and striatum. Eur J Drug Metab Pharmacokinet 25: 79–84.

Gudelsky GA, Nansel DD, Porter JC (1981). Role of estrogen in the dopaminergic control of prolactin secretion. Endocrinology 108: 440–444.

Harding SD, Sharman JL, Faccenda E, Southan C, Pawson AJ, Ireland S *et al*. (2018). The IUPHAR/BPS guide to pharmacology in 2018: updates and expansion to encompass the new guide to immunopharmacology. Nucl Acids Res 46: D1091–D1106.

Hurko O, Ryan JL (2005). Translational research in central nervous system drug discovery. NeuroRx 2: 671–682.

Ishibashi M, Yamaji T (1981). Direct effects of thyrotropin-releasing hormone, cyproheptadine, and dopamine on adrenocorticotropin secretion from human corticotroph adenoma cells in vitro. J Clin Invest 68: 1018–1027.

Ishibashi M, Yamaji T (1984). Direct effects of catecholamines, thyrotropin-releasing hormone, and somatostatin on growth hormone and prolactin secretion from adenomatous and nonadenomatous human pituitary cells in culture. J Clin Invest 73: 66–78.

Jonker DM, Visser SAG, van der Graaf PH, Voskuyl RA, Danhof M (2005). Towards a mechanism-based analysis of pharmacodynamic drug-drug interactions *in vivo*. Pharmacol Ther 106: 1–18.

Khandelwal A, Harling K, Jonsson EN, Hooker AC, Karlsson MO (2011). A fast method for testing covariates in population PK/PD models. AAPS J 13: 464–472.

Kilkenny C, Browne W, Cuthill IC, Emerson M, Altman DG (2010). Animal research: reporting *in vivo* experiments: the ARRIVE guidelines. Br J Pharmacol 160: 1577–1579.

Kurashima M, Domae M, Inoue T, Nagashima M, Yamada K, Shirakawa K *et al*. (1996). Inhibitory effects of putative dopamine D_3 receptor agonists, 7-OH-DPAT and quinpirole, on prolactin secretion in rats. Pharmacol Biochem Behav 53: 379–383.

Li H, Yan Z (2010). Analysis of amino acid neurotransmitters in hypothalamus of rats during cerebral ischemia–reperfusion by microdialysis and capillary electrophoresis. Biomed Chromatogr 24: 1185–1192 https://doi.org/10.1002/bmc.1425.

Liang S, Hsu S, Pan J (2014). Involvement of dopamine D_2 receptor in the diurnal changes of tuberoinfundibular dopaminergic neuron activity and prolactin secretion in female rats. J Biomed Sci 21: 1–9.

Liang S, Pan J (2012). An endogenous dopaminergic tone acting on dopamine D_3 receptors may be involved in diurnal changes of tuberoinfundibular dopaminergic neuron activity and prolactin secretion in estrogen-primed ovariectomized rats. Brain Res Bull 87: 334–339.

Lyons DJ, Broberger C (2014). TIDAL WAVES: network mechanisms in the neuroendocrine control of prolactin release. Front Neuroendocrinol 35: 420–438.

McGrath JC, Lilley E (2015). Implementing guidelines on reporting research using animals (ARRIVE etc.): new requirements for publication in BJP. Br J Pharmacol 172: 3189–3193.

Millan MJ, Maiofiss L, Cussac D, Audinot V, Boutin J-A, Newman-Tancredi A (2002). Differential actions of antiparkinson agents at multiple classes of monoaminergic receptor. I. A multivariate analysis of the binding profiles of 14 drugs at 21 native and cloned human receptor subtypes. J Pharmacol Exp Ther 303: 791–804.

Morel GR, Carónc RW, Cónsoleb GM, Soajec M, Sosa YE, Rodríguez SS *et al*. (2009). Estrogen inhibits tuberoinfundibular dopaminergic neurons but does not cause irreversible damage. Brain Res Bull 80: 347–352.

Movin-Osswald G, Hammarlund-Udenaes M (1995). Prolactin release after remoxipride by an integrated pharmacokinetic-pharmacodynamic model with intra- and interindividual aspects. J Pharmacol Exp Ther 274: 921–927.

Petersson KJ, Vermeulen AM, Friberg LE (2013). Predictions of *in vivo* prolactin levels from in vitro K_i values of D_2 receptor antagonists using an agonist–antagonist interaction model. AAPS J 15: 533–541.

Petty RG (1999). Prolactin and antipsychotic medications: mechanism of action. Schizophr Res 35: 67–73.

Pivonello R, Ferone D, Lombardi G, Colao A, Lamberts SWJ, Hofland LJ (2007). Novel insights in dopamine receptor physiology. Eur J Endocrinol 156: S13–S21.

Schoemaker RC, van Gerven JM, Cohen AF (1998). Estimating potency for the E_{max}-model without attaining maximal effects. J Pharmacokinet Biopharm 26: 581–593.

Shimizu S, den Hoedt SM, Mangas-sanjuan V, Cristea S, Geuer JK, van den Berg D *et al*. (2017). Target-site investigation for the plasma prolactin response: mechanism-based pharmacokinetic-pharmacodynamic analysis of risperidone and paliperidone in the rats. Drug Metab Dispos 45: 152–159.

Soares HD (2010). The use of mechanistic biomarkers for evaluating investigational CNS compounds in early drug development. Curr Opin Investig Drugs 11: 795–801.

Stevens J, Ploeger BA, Hammarlund-Udenaes M, Osswald G, van der Graaf PH, Danhof M *et al*. (2012). Mechanism-based PK-PD model for the prolactin biological system response following an acute dopamine inhibition challenge: quantitative extrapolation to humans. J Pharmacokinet Pharmacodyn 39: 463–477.

Taneja A, Vermeulen A, Huntjens DRH, Danhof M, De Lange ECM, Proost JH (2016). A comparison of two semi-mechanistic models for prolactin release and prediction of receptor occupancy following administration of dopamine D_2 receptor antagonists in rats. Eur J Pharmacol 789: 202–214.

Tirelli E, Jodogne C (1993). Behavioral sensitization and tolerance to the D_2 agonist RU 24213: dissociation between several behavior patterns in mice. Pharmacol Biochem Behav 44: 627–632.

Tuomisto J, Mannisto P (1985). Neurotransmitter regulation of anterior pituitary hormones. Pharmacol Rev 37: 249–332.

van den Brink WJ, Wong YC, Gülave B, van der Graaf PH, de Lange ECM (2017). Revealing the neuroendocrine response after remoxipride treatment using multi-biomarker discovery and quantifying it by PK/PD modeling. AAPS J 19: 274–285.

van der Greef J, Martin S, Juhasz P, Adourian A, Plasterer T, Verheij ER (2007). The art and practice of systems biology in medicine: mapping patterns of relationships. J Proteome Res 6: 1540–1559.

van der Greef J, Mcburney RN (2005). Rescuing drug discovery: *in vivo* systems pathology and systems pharmacology. Nat Rev Drug Discov 4: 961–968.

Vance MLEE, Kaiser DL, Frohman LA, Rivier J, Vale WW, Thorner MO (1987). Role of dopamine in the regulation of growth hormone secretion: dopamine and bromocriptine augment growth hormone (GH)-releasing hormone-stimulated GH secretion in normal man. J Clin Endocrinol Metab 64: 1136–1141.

Viswanathan CT, Bansal S, Booth B, DeStefano AJ, Rose MJ, Sailstad J *et al*. (2007). Quantitative bioanalytical methods validation and implementation: best practices for chromatographic and ligand binding assays. Pharm Res 24: 1962–1973.

Westerhout J, Ploeger B, Smeets J, Danhof M, de Lange ECM (2012). Physiologically based pharmacokinetic modeling to investigate regional brain distribution kinetics in rats. AAPS J 14: 543–553.

Yamamoto Y, Välitalo PA, van den Berg D-J, Hartman R, van den Brink WJ, Wong YC *et al*. (2016). A generic multi-compartmental CNS distribution model structure for 9 drugs allows prediction of human brain target site concentrations. Pharm Res 34: 333–351.

Supporting Information

Additional supporting information may be found online in the Supporting Information section at the end of the article.

https://doi.org/10.1111/bph.14452

Figure S1 (A) Visualization of the automated model selections for the baseline model (A) and the PK/PD model (B) on basis of adjusted objective function value (suppl. Equations part I, 8). Grey dots represent the adjusted objective function value for each evaluated model, while blue dots represent the selected models.

Figure S2 Visual predictive check of the quinpirole PK/PD models for ACTH, GH, prolactin (PRH) and TSH at experiment day 1 and 8. The colored dots represent the observed data, with the solid colored lines showing the mean of the observations. The solid grey line shows the mean, and the dashed grey lines the 90% confidence interval of 500 simulations.

Figure S3 A) Simulated concentration-effect relations for ACTH (black), TSH (green), GH (red) and prolactin (PRH; blue) on basis of the parameter estimates in table III as compared to the fits by the operational model (equation 1). Each figure represents a different scenario with regard to the hormones included in the relation between tau and D_2 receptor expression (equation 2). The signal transduction efficiency τ is assumed dependent on pituitary D_2 receptor expression for the hormones indicated above each figure. For the hormone not included, the signal transduction efficiency τ is estimated separately.

Table S1 Parameter estimates for ACTH, prolactin (PRH) and TSH with and without covariate effect.

Data S1 Supplementary Methods.

Data S2 Supplementary Equations.